sphere [reviewed in (*12-14*)]. During the outbound pass the 5-hour periodicity suggests on the one hand that a rigidly rotating magnetodisk (*2*) is probably a viable model to a distance of ~ 85 R_J, and perhaps to ~ 130 R_J. On the other hand, the data could be consistent with a "warped" disk beyond ~ 85 R_J (*15*). Since neutral sheet crossings were not seen after day 69 (*11*), one would expect that the difference in longitude between the dipole axis and the observed intensity peaks would be about 180°. We find the intensity peaks tend to occur at about 90° to 130° longitude (System III), while the dipole axis is located at about 200° longitude, a difference of 90°. This seems to be at variance with the magnetodisk model. A 10-hour periodicity is predicted by the magnetic anomaly model (*13*). The relation between the particle enhancements at about 90° longitude and the magnetic anomaly at about 230° longitude is not known. Finally, no evidence was found in the magnetosphere inside the magnetopause for radial outflow of hot plasma on either the inbound or outbound passes, indicating that a "planetary wind" or "breeze" (*16*) was not operating at Jupiter during the Voyager 1 passage. Flow directions in Fig. 7 are consistent with convective flow (*12*) which could be a combination of corotational and field-aligned components resulting in an overall sunward vector.

S. M. KRIMIGIS
Applied Physics Laboratory, Johns Hopkins University, Laurel, Maryland 20810
T. P. ARMSTRONG
Department of Physics and Astronomy, University of Kansas, Lawrence 66044
W. I. AXFORD
Max-Planck Institute for Aeronomy, D-3411 Katlenburg-Lindau 3, West Germany
C. O. BOSTROM
Applied Physics Laboratory, Johns Hopkins University
C. Y. FAN
Department of Physics, University of Arizona, Tucson 85721
G. GLOECKLER
Department of Physics and Astronomy, University of Maryland, College Park 20742
L. J. LANZEROTTI
Bell Telephone Laboratories, Murray Hill, New Jersey 07974
E. P. KEATH, R. D. ZWICKL
J. F. CARBARY
Applied Physics Laboratory, Johns Hopkins University
D. C. HAMILTON
Department of Physics and Astronomy, University of Maryland

References and Notes

1. S. M. Krimigis, T. P. Armstrong, W. I. Axford, C. O. Bostrom, C. Y. Fan, G. Gloeckler, L. J. Lanzerotti, *Space Sci. Rev.* **21**, 329 (1977).
2. J. A. Van Allen, D. N. Baker, B. A. Randall, M. F. Thomsen, D. D. Sentman, H. R. Flindt, *Science* **183**, 309 (1974).
3. J. A. Simpson *et al.*, *ibid.*, p. 306; J. H. Trainor, B. J. Teegarden, D. E. Stilwell, F. B. McDonald, E. C. Roelof, W. R. Webber, *ibid.*, p. 311.
4. N. Divine, *JPL IOM 3574-78-171* (1978).
5. R. W. Fillius, *Jupiter*, T. Gehrels, Ed. (Univ. of Arizona Press, Tucson, 1976), p. 896.
6. D. J. Williams, *J. Geophys. Res.* **84**, 101 (1979).
7. F. M. Ipavich, *Geophys. Res. Lett.* **1**, 149 (1974); R. E. Gold, C. O. Bostrom, E. C. Roelof, D. J. Williams, *Proceedings of the 14th International Cosmic Ray Conference (Munich)* (Max Planck Institute for Extraterrestrial Physics, Munich, 1975), p. 1801.
8. F. L. Scarf, D. A. Gurnett, W. S. Kurth, *Science* **204**, 991 (1979).
9. T. V. Johnson, *Annu. Rev. Earth Planet. Sci.* **6**, 93 (1978).
10. J. A. Van Allen and N. F. Ness, *J. Geophys. Res.* **74**, 71 (1969).
11. N. F. Ness, M. H. Acuña, K. W. Behannon, R. P. Lepping, L. F. Burlaga, F. M. Neubauer, *Science* **204**, 982 (1979).
12. N. M. Brice and G. A. Ioannides, *Icarus* **13**, 173 (1970).
13. A. J. Dessler and V. M. Vasyliunas, *Geophys. Res. Lett* **6**, 37 (1979).
14. C. F. Kennel and F. V. Coroniti, *Annu. Rev. Astron. Astrophys.* **15**, 389 (1977).
15. M. G. Kivelson, P. J. Coleman, Jr., L. Froidevaux, R. L. Rosenberg, *J. Geophys. Res.* **83**, 4823 (1978).
16. F. C. Michel and P. A. Sturrock, *Planet. Space Sci.* **22**, 1501 (1974).
17. D. Hovestadt, G. Gloeckler, C. Y. Fan, L. A. Fisk, F. M. Ipavich, B. Klecker, J. J. O'Gallagher, M. Scholer, *Geophys. Res. Lett.* **5**, 1055 (1978).
18. G. Gloeckler, *Rev. Geophys. Space Phys.*, in press.
19. G. L. Withbroe, *Natl. Bur. Stand. (U.S.) Spec. Publ.* **353**, 127 (1971).
20. A. G. W. Cameron, *Space Sci. Rev.* **15**, 121 (1970).
21. S. J. Bame, J. R. Asbridge, W. C. Feldman, J. T. Gosling, *J. Geophys. Res.* **82**, 1487 (1977).
22. We thank the Voyager Project Office, JPL, and the Planetary Programs Office, NASA Headquarters, for their assistance with this experiment. We are grateful to D. P. Peletier, S. A. Gary, R. G. King, J. W. Kohl, D. E. Fort, J. T. Mueller, J. H. Crawford, R. E. Thompson, B. A. Northrop, and J. Hook at JHU/APL, to J. Cain, E. Tums, and R. Lundgren of the University of Maryland, to C. G. Maclennan of Bell Laboratories, and to P. R. Briggs, R. B. Decker, S. T. Branden, J. H. Nonnast, F. Kutchko, M. Paonessa, and J. O'Donnell of the University of Kansas for their help in making the LECP experiment a success. The work of E. Franzgrote and D. Griffith of JPL (among many others) was essential to the success of our investigation. The LECP program was supported at JHU/APL by NASA under Task I of contract N00024-78-C-5384 between the Johns Hopkins University and the Department of the Navy and by subcontract at the universities of Kansas, Maryland, and Arizona. This report presents the results of one phase of research carried out with JPL under NASA contract NAS 7-100.

24 April 1979

Voyager 1: Energetic Ions and Electrons in the Jovian Magnetosphere

Abstract. *The observations of the cosmic-ray subsystem have added significantly to our knowledge of Jupiter's magnetosphere. The most surprising result is the existence of energetic sulfur, sodium, and oxygen nuclei with energies above 7 megaelectron volts per nucleon which were found inside of Io's orbit. Also, significant fluxes of similarly energetic ions reflecting solar cosmic-ray composition were observed throughout the magnetosphere beyond 11 times the radius of Jupiter. It was also found that energetic protons are enhanced by 30 to 70 percent in the active hemisphere. Finally, the first observations were made of the magnetospheric tail in the dawn direction out to 160 Jupiter radii.*

The observations of the cosmic-ray subsystem (CRS) experiment during the Jovian flyby of Voyager 1 have added significantly to our knowledge of Jupiter's giant and dynamic magnetosphere and its complex relationship to the solar wind and the Jovian moons. Here we present data on the spatial and temporal intensity variations of electrons and protons, the flow patterns of the protons, and the ion composition from lithium through iron. These data confirm and extend much of the morphology reported by the Pioneer 10 and 11 investigators of a chaotic outer region dominated by azimuthal asymmetries and temporal variations with an equatorial current sheet, large field-aligned streaming of the energetic protons, and the occasional presence of a planetary wind in the more distant regions (*1-3*). Inside 20 Jupiter radii (R_J) a classical magnetosphere prevails with durable trapping but with the added complexity of the sweeping effects of the Jovian moons. The CRS experiment measures the three-dimensional flow pattern of the energetic ions as well as their detailed composition. Furthermore, the near-equatorial trajectory allowed measurements on both sides of the current-sheet region.

The instrument consists of seven multielement particle telescopes that are designed primarily to study the charge and energy spectra of low and medium energy galactic cosmic rays (*4*). During portions of the encounter, many systems were saturated by the high counting rates. Those data have either been corrected or eliminated from this discussion.

Energetic particle morphology. A small solar proton event, with no associated increase in nuclei with charge $Z \geq 6$, was in progress prior to the first bow shock encounter at 85.6 R_J, and the primary flow direction of energetic protons (0.4 to 8 MeV) was toward Jupiter.

Near the bow shock and in the magnetosheath (5, 6) the low energy proton flux increased by a factor of 2 to 4, with an outward flow toward the dawnside between 90° and 180° azimuth (Fig. 1). Once Voyager entered the magnetosphere at 66.9 R_J, both electron and proton fluxes increased by at least an order of magnitude and the proton intensities were within a factor of 2 of those observed earlier by Pioneer 11 in this region. Proton anisotropies were large but variable and the general flow pattern was away from Jupiter. Such an outflow can be caused not only by a planetary wind (2, 3) but also by a diffusionlike process at higher energies. A number of magnetosphere and bow shock crossings were encountered between 66.9 and 46.6 R_J. This period is characterized by large anisotropies and variable flow directions.

The second entry at 46.6 R_J was into the midmagnetosphere which corotates with Jupiter, and therefore one expects a unidirectional particle anisotropy in the corotation direction (azimuth of 270°). At 45 R_J, this anisotropy should be about 40 percent for 0.5-MeV protons and decrease nearly linearly with decreasing radial distance. Between 40 and 45 R_J both the magnitude and direction of the observed anisotropy agree with this simple picture, but as with the Pioneer 10 results (3), the magnitude exceeds the corotation value between 20 and 37 R_J and is probably indicative of field-aligned streaming.

In the midmagnetosphere, particle intensities on Pioneer 10 dropped off by at least a factor of 2 at 8° from the magnetic equator (1, 3). Because of the ~ 10° offset between the magnetic dipole and spin axis, Voyager crossed the magnetic equator twice every 10 hours at longitudes of approximately 100° and 300° (λ_{III}, 1965). At these crossings the > 0.4-MeV proton flux was two to four times as large as observed with Pioneer 10. Proton fluxes observed at the $\lambda_{III} \approx 300°$ crossings (inside of 40 R_J) were 30 to 70 percent more intense than those at $\lambda_{III} \approx 100°$. Thus the trapped proton fluxes are larger in the active hemisphere (7-9). The peaks observed at $\lambda_{III} \sim 250°$ and 320° in Fig. 2 can also be associated with the active hemisphere. In this region, the sweeping effects of Io and Europa are also evident.

Both the Voyager 1 and Pioneer 10 outbound passes (≈ 120° and 90°, respectively, toward dawn from the Jupiter-sun direction) encountered a thin plasma sheet (6) around which the energetic electron and proton populations were confined (Fig. 3). Since the jovicentric latitude of Voyager 1 was only a few degrees (3° at 20 R_J and 5° at 150 R_J), Voyager crossed the calculated dipole equator twice each 10 hours, corresponding to $\lambda_{III} \approx 95°$ and 310°. Again, the fluxes between 20 and 40 R_J in the active hemisphere were significantly more intense than in the inactive hemisphere. Figure 3, inset A, shows the spacecraft longitude plotted against distance when the major proton flux maxima occurred (> 0.4 MeV). Maxima in the active hemisphere exhibit a steady

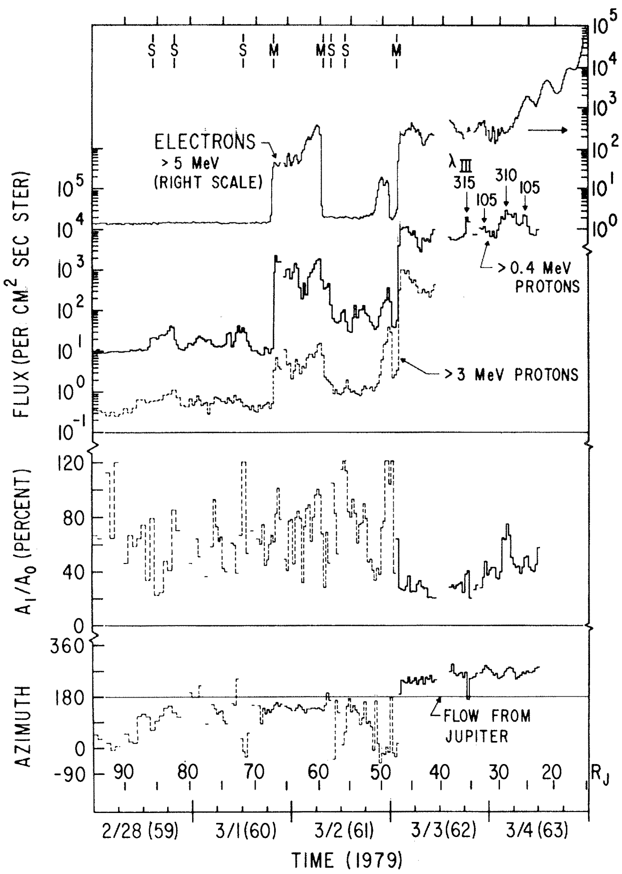

Fig. 1. Flux (16-minute averages) of electrons (intensity scale at right) and flux (32-minute averages) of protons (left intensity scale) observed during the inbound pass of Voyager 1. The lower panels give the magnitude and azimuth (in the ecliptic plane) of the first order anisotropy $\mathbf{A}_1$ of the proton flux, where A_0 is the omnidirectional component (16). Azimuths of 0° and 180° correspond to flow toward and away from Jupiter; flow in the corotation direction is observed at 270°. The dashed curves correspond to > 3-MeV protons and the solid curves to > 0.4 MeV. Bow shock and magnetosphere crossings (5) are indicated by S and M, respectively. Jovicentric longitudes (λ_{III}) of flux maxima near magnetic equatorial crossings are indicated.

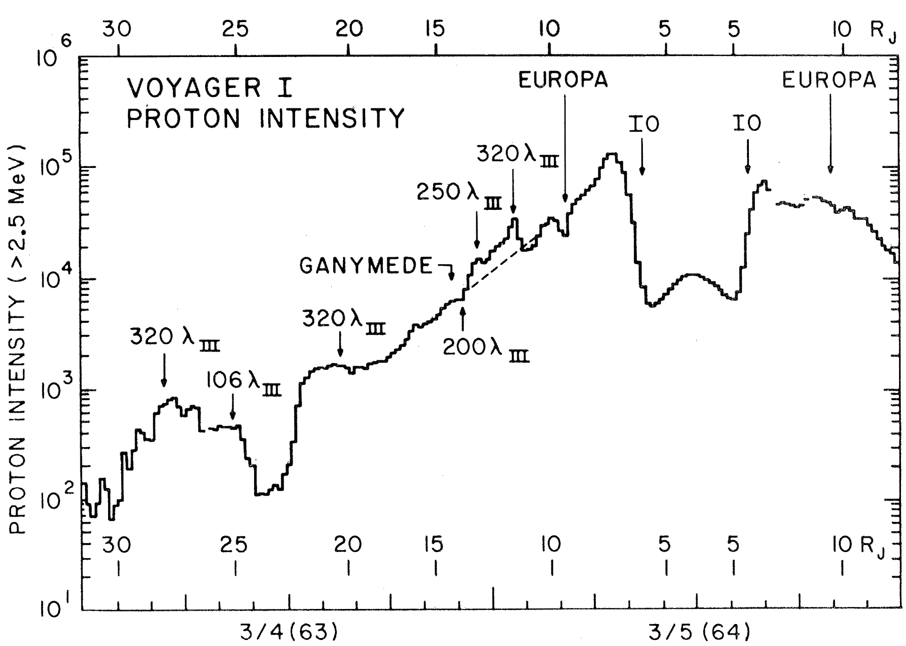

Fig. 2. Approximate intensity (per square centimeter per second per steradian, 16-minute averages) of protons (> 2.5 MeV) observed inside 30 R_J. Due to the extreme fluxes, the detector threshold shifted with counting rate and the part of the spectrum sampled changed somewhat during this part of the trajectory.

phase delay of 1 hour (36° in λ_{III}) per 27 R_J, thus indicating a rigid rotation of a warped magnetic equator. The phases of the inactive hemisphere maxima, however, are quite variable and not well organized inside 80 R_J.

Outside 80 R_J the spacecraft probably did not cross the plasma sheet, but just dipped into its upper edge once every 10 hours when the sheet was at maximum jovicentric latitude. The maxima should thus have occurred when the north dipole was tipped away from the spacecraft (that is, when the spacecraft was at $\lambda_{III} = 20°$), with a phase shift due to the finite outward propagation speed of the rotational perturbation. The upper straight line in Fig. 3, inset A, which corresponds to $\lambda_{III} = 20°$ at 20 R_J and a phase delay of 1 hour per 32 R_J, fits the location of the maxima beyond 80 R_J. These delays are comparable to those observed by Pioneer 10 (*10*).

Proton anisotropies and flow directions during the outbound pass were variable. The dominant anisotropy was in the corotation direction with (beyond 50 R_J) a substantial component of flow toward Jupiter. Such a component might be expected if the observations occurred during the recovery phase of a magnetic storm. Most of the time, in particular between 100 and 130 R_J, the anisotropy was from south toward north as would be expected if the plasma sheet and maximum flux were south of the spacecraft. Beyond ~ 140 R_J as Voyager 1 approached the magnetopause, the intensity of electrons and low energy protons increased again and exhibited variations that were quite different from those associated with the current sheet.

Table 1. Elemental abundances of energetic heavy nuclei (relative to oxygen ≡ 1).

Element	Atomic number Z	Solar system abundances*	Solar energetic particle abundances†	Jovian abundances‡	
				Outer region§	Inner region‖
C	6	0.571 ± 0.197	0.35 to 0.54	0.55 ± 0.13	≤ 0.03
N	7	$0.114^{+0.074}_{-0.051}$	0.11 to 0.13	≤ 0.06	≤ 0.07
O	8	1	1	1	1
Ne	10	0.081 ± 0.039	0.11 to 0.24	$0.09^{+0.06}_{-0.04}$	≤ 0.01
Na	11	0.0025 ± 0.0007	0.01 to 0.02	≤ 0.04	0.04 ± 0.02
Mg	12	0.050 ± 0.012	0.16 to 0.29	$0.13^{+0.07}_{-0.05}$	≤ 0.03
Si	14	0.048 ± 0.011	0.11 to 0.31	$0.11^{+0.07}_{-0.05}$	≤ 0.02
S	16	0.019 ± 0.008	0.02 to 0.07	$0.04^{+0.05}_{-0.03}$	0.76 ± 0.09
K	19	0.00016 ± 0.00006	≤ 0.0075	≤ 0.04	≤ 0.01
Fe	26	0.041 ± 0.010	0.04 to 0.63	$0.06^{+0.06}_{-0.03}$	≤ 0.01

*After Meyer and Reeves (*15*). †Range of values measured with the Voyager cosmic ray instrument for six flares, September 1977 to May 1978. Energy 8.5 to 14 MeV per nucleon. ‡Energy (megaelectron volts per nucleon) for C through S, 7 to 14; for K, 7.2 to 14; for Fe, 7.6 to 14. Upper limits (≤) are at 84 percent confidence level. §Time (UT): 1 March 1979, 2006 to 5 March 1979, 0202 and 6 March 1979, 0256 to 12 March 1979, 0042. ‖Time (UT): 5 March 1979, 1100 to 5 March 1979, 1200

Energetic particle elemental composition. The elemental composition and energy spectra of energetic trapped particles are a key to the identification of the plasma source (for example, solar wind, solar flares, ionosphere, Jovian moons) which feeds the magnetospheric acceleration process as well as to the understanding of the nature of the acceleration process itself. We report here the first measurements of ≥ 7 MeV per nucleon particles with charge $Z > 2$ in the Jovian magnetosphere.

The observed elemental composition is shown in Fig. 4b for the middle and outer magnetosphere (> 11 R_J) and in Fig. 4a for the inner magnetosphere. The charge Z of each event is determined uniquely by a three-parameter double dE/dx-E technique for particles stopping in the low energy telescopes (LET's) (*4*). The resulting resolution ($0.1 \le \sigma_Z \le 0.3$) allows detailed charge spectra to be ob-

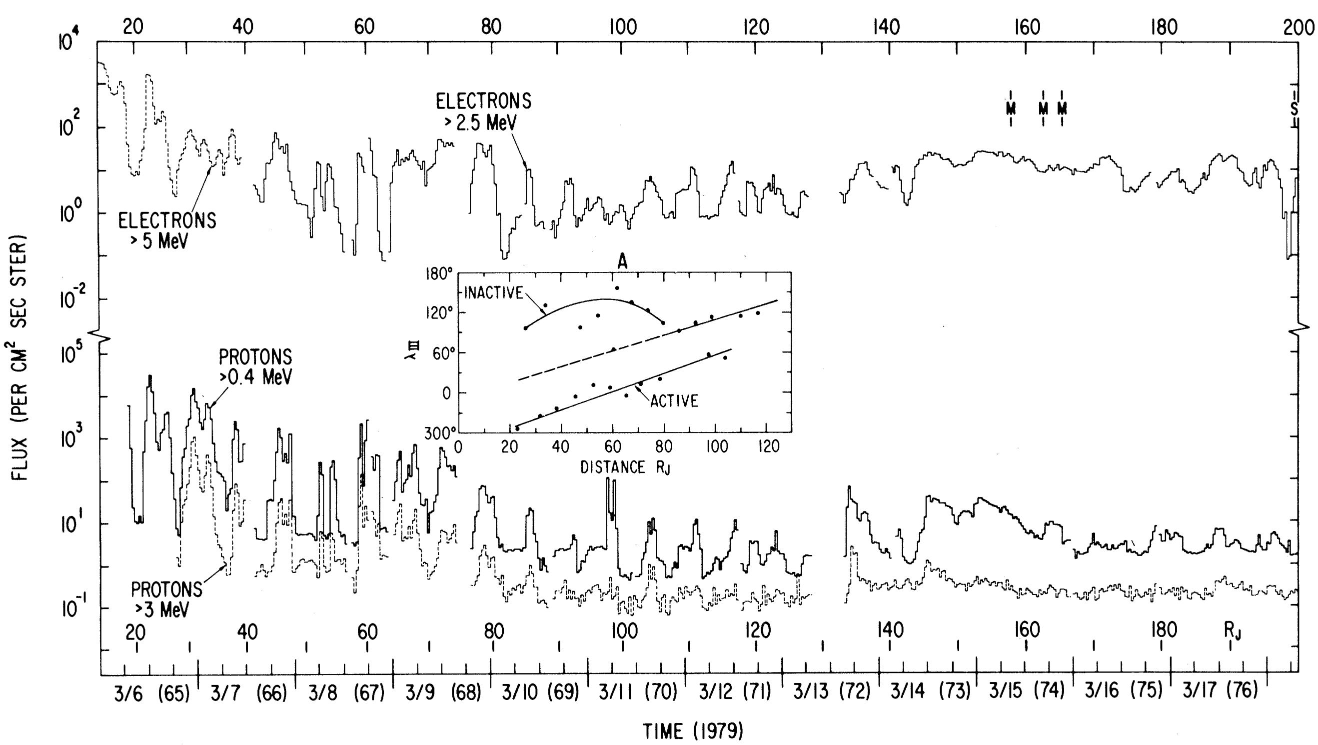

Fig. 3. Electron and proton fluxes (32-minute averages) observed during the Voyager 1 outbound pass into the dawn sector of the magnetospheric tail at ~ 120° to the Jupiter-sun line. Bow shock and magnetopause crossings (*5*) indicated by S and M. (Inset A) Voyager 1 longitude (λ_{III}) corresponding to major maxima in the > 0.4-MeV proton flux. Maxima corresponding to the active and inactive hemispheres show a distinctly different phase lag versus radial distance.

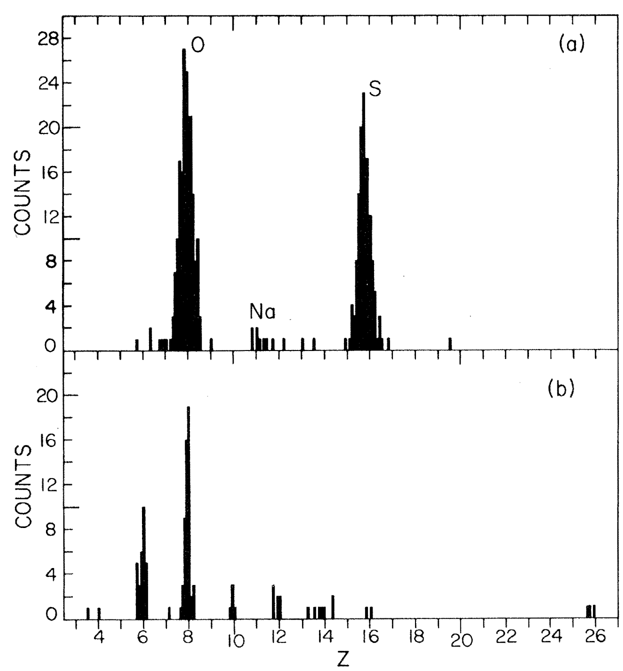

Fig. 4. Measured element (Z) distribution for heavy nuclei in the Jovian environment. (a) Within ~ 5.8 R_J (inner region, see Table 1). (b) Outside ~ 11 R_J (outer region, see Table 1).

tained for helium through iron. The two observed populations are distinctly different; beyond 11 R_J the even-numbered elements C, O, Ne, Mg, Si, and Fe are evident (Fig. 4b), while in the inner region ($< 5.8\ R_J$) O and S dominate with Na also being clearly evident (Fig. 4a).

To improve statistics in the outer region, we included the events observed just outside the magnetosphere. Detailed comparisons of the abundances are consistent with the identification of events observed on 2 March 1979 as particles which have leaked out of the magnetosphere following the compression and inward motion of the magnetopause which occurred on that day (*5, 6*).

Table 1 shows the marked similarity of the composition in the outer region and in solar energetic particles. Comparison with solar system abundances shows that the outer region composition is modestly enhanced in Mg, Si, and possibly S. It is unlikely that the Jovian ionosphere or the Galilean satellites are the source of these particles, since Jupiter and the satellites are highly differentiated and the resulting composition should be highly nonsolar. Although these particles could have been transient solar particles which had penetrated deep into the magnetosphere, there is no evidence just prior to encounter that such a transient increase of solar particles with $Z \geq 6$ occurred. However, durable trapping of particles from previous solar flares cannot now be ruled out in the outer Jovian magnetosphere. Such a dynamical trapping process would be another unique characteristic of the Jovian magnetosphere, since it is unlikely that such trapping occurs in Earth's magnetosphere (*11*). Alternatively, the solar wind may be the source of plasma which is eventually accelerated to high energies as is thought to be the case for Earth (*12*).

As the orbit of Io is approached the composition changes dramatically (Fig. 5) with O, Na, and S becoming the dominant elements. Note that O, Na, and S are not uniformly distributed; for example, Na appears to be concentrated during a 1-hour interval at the magnetic equator (1100 to 1200 universal time).

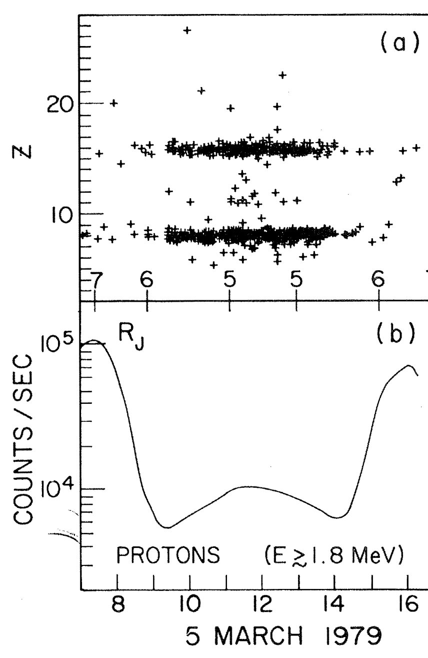

Fig. 5. (a) Observations of energetic nuclei near Jupiter as a function of spacecraft time [hours Universal Time (UT)] and jovicentric radial distance (R_J). Each symbol (+) represents the measurement of a nucleus of element Z. Because of rapidly changing counting linetime before 0930 and after 1400 hours, the spatial extent of the enhanced O and S fluxes is not accurately represented by this figure. (b) Counting rate profile of energetic protons versus UT and R_J.

Comparison of the elemental abundances of this inner region with those of the solar system (Table 1 and Fig. 4a) indicates that O is enhanced by a factor of ≥ 17 with respect to C, Na by a factor of ≥ 270, and S by a factor of ≥ 700. The overabundance of O and S is qualitatively consistent with the composition of the Io plasma torus (*6*), suggesting Io as their source. Similarly, the ionization (*13*) of the neutral Na cloud associated with Io is a likely source for the anomalous Na.

The absence outside of 11 R_J of enhanced O, Na, and S with $E > 7$ MeV per nucleon requires that the acceleration of the torus plasma to high energies occurs inside that radius. Further analysis of the data is needed to determine whether the acceleration occurs only within Io's orbit and what effect Io's sweeping has on the diffusion of high energy O, Na, and S from the inner to the outer region. Thus the relationship of ≥ 7 MeV per nucleon element enhancements to the 0.3 to 0.5 MeV per nucleon S as observed in the outer magnetosphere (*14*) is undetermined. If Io is indeed the source of the enhanced ≥ 7 MeV per nucleon O, Na, and S, and if the acceleration takes place inside Io's orbit, the mechanism has to result in a substantial population of high energy particles only a short distance from the source, which may require processes other than or in addition to radial diffusion.

R. E. Vogt, W. R. Cook
A. C. Cummings, T. L. Garrard
N. Gehrels, E. C. Stone
California Institute of Technology, Pasadena 91125
J. H. Trainor, A. W. Schardt
T. Conlon, N. Lal
F. B. McDonald
NASA Goddard Space Flight Center, Greenbelt, Maryland 20771

References and Notes

1. See relevant articles in *Jupiter*, T. Gehrels, Ed., (Univ. of Arizona Press, Tucson, 1976).
2. C. F. Kennel and F. V. Coroniti, *Annu. Rev. Astron. Astrophys.* **15**, 389 (1977).
3. F. B. McDonald, A. W. Schardt, J. H. Trainor, *J. Geophys. Res.* in press.
4. E. C. Stone, R. E. Vogt, F. B. McDonald, B. J. Teegarden, J. H. Trainor, J. R. Jokipii, W. R. Webber, *Space Sci. Rev.* **21**, 355 (1977).
5. N. F. Ness, M. H. Acuña, R. P. Lepping, L. F. Burlago, K. W. Behannon, F. M. Neubauer, *Science* **204**, 982 (1979).
6. H. S. Bridge, J. W. Belcher, A. J. Lazarus, J. D. Sullivan, R. McNutt, F. Bagenal, J. D. Scudder, E. C. Sittler, *ibid.*, p. 987.
7. V. M. Vasyliunas, *Geophys. Res. Lett.* **2**, 87 (1975).
8. A. J. Dessler, *ibid.* **5**, 65 (1978).
9. ______ and V. M. Vasyliunas, *ibid.* **6**, 37 (1979).
10. M. G. Kivelson, P. J. Coleman, Jr., L. Froide-

vaux, R. L. Rosenberg, *J. Geophys. Res.* **83**, 4823 (1978).
11. J. B. Blake and G. A. Paulikas, *ibid.* **77**, 3431 (1972).
12. D. Hovestadt, G. Gloeckler, C. Y. Fan, L. A. Fisk, F. M. Ipavich, B. Klecker, J. J. O'Gallagher, M. Scholer, *Geophys. Res. Lett.* **5**, 1055 (1978).
13. R. W. Carlson, D. L. Matson, T. V. Johnson, *ibid.* **2**, 469 (1975).
14. S. M. Krimigis *et al.*, *Science* **204**, 998 (1979).
15. J. P. Meyer and H. Reeves, *Proceedings of the 15th International Cosmic Ray Conference Plovdiv, Bulgaria* **2**, 137 (1977).
16. For first-order anisotropy the intensity I_n in the nth LET telescope can be expressed as

$$I_n = A_0 - \mathbf{A}_1 \cdot \hat{\mathbf{T}}_n$$

where $\hat{\mathbf{T}}_n$ is a unit vector along the viewing direction of the telescope. Two of the telescopes are aligned with their viewing directions opposite each other; the remaining two are orthogonal to each other and to the other pair. The resulting set of four linear equations can be solved for A_0 and the three components of $\mathbf{A}_1$.
17. We thank the Voyager Project and the enthusiastic staff of our laboratories at California Institute of Technology (Caltech) and Goddard Space Flight Center (GSFC) for splendid support. Special thanks go to W. Althouse (Caltech), W. Davis, H. Domchick, and D. Stilwell (GSFC), and E. Franzgrote (JPL), who had major responsibilities. Supported by NASA under contracts NAS 7-100 and NGR 05-002-160.

23 April 1979

Infrared Images of Jupiter at 5-Micrometer Wavelength During the Voyager 1 Encounter

Abstract. *A coordinated program to observe Jupiter at high spatial resolution in the 5-micrometer wavelength region was undertaken to support Voyager 1 imaging and infrared radiation experiment targeting. Jupiter was observed over a 5-month period from Palomar and Mauna Kea observatories. The frequency of observations allowed the selection of interesting areas for closer Voyager examination and also provided good short-term monitoring of variations in cloud morphology. Significant global changes in the 5-micrometer distribution are seen over this time period.*

Gillett *et al.* (*1*) discovered enhanced infrared radiation at wavelengths near 5 μm from the central regions of Jupiter's disk, and Westphal (*2*) showed that this thermal radiation originates in localized areas, principally in the equatorial regions. Infrared images of Jupiter at 5 μm, made by scanning a single detector across the planet, were obtained by other investigators (*3*), including Terrile (*4*) who analyzed a 4-year series of these data to show that there are at least three different cloud layers in Jupiter's atmosphere, each characterized by a distinct brightness temperature. The regions of highest 5-μm flux are the deepest observable levels in the planet's atmosphere and correspond to the blue-gray areas in Jovian belts (*5*). The white zones and Great Red Spot are the coldest 5-μm regions.

Voyager 1 afforded an opportunity to make spectroscopic and radiometric observations with high spectral resolution and sufficient spatial resolution to include individual hot regions. In order to predict the global 5-μm appearance of Jupiter at the time of Voyager encounter and the location of specific hot spots for spacecraft observations, we undertook a program of 5-μm imagery of the planet in September 1978 and continued the ground-based observations through the time of Voyager 1 encounter. Terrile (*4*, *6*) had found that the gross appearance of Jupiter changes from year to year, and that while some regions of enhanced 5-μm emission have lifetimes of several months, others form and dissipate on a time scale of days. Planning and sequencing considerations for spacecraft observations at near-encounter required that 5-μm hot spot targets be established with a high degree of certainty as to position and expected degree of "activity" at least 1 month in advance of the encounter date.

Observations were made throughout the apparition of Jupiter with the 5-m Hale telescope at Palomar Mountain and with the 2.24-m telescope at Mauna Kea Observatory in Hawaii in a cooperative program (coordinated by R.J.T.). The technique for observing and image reconstruction has been described (*5*). Observations were obtained at each observatory in blocks of 2 to 5 nights each separated by 2 to 3 weeks starting in September 1978 and continuing through March 1979.

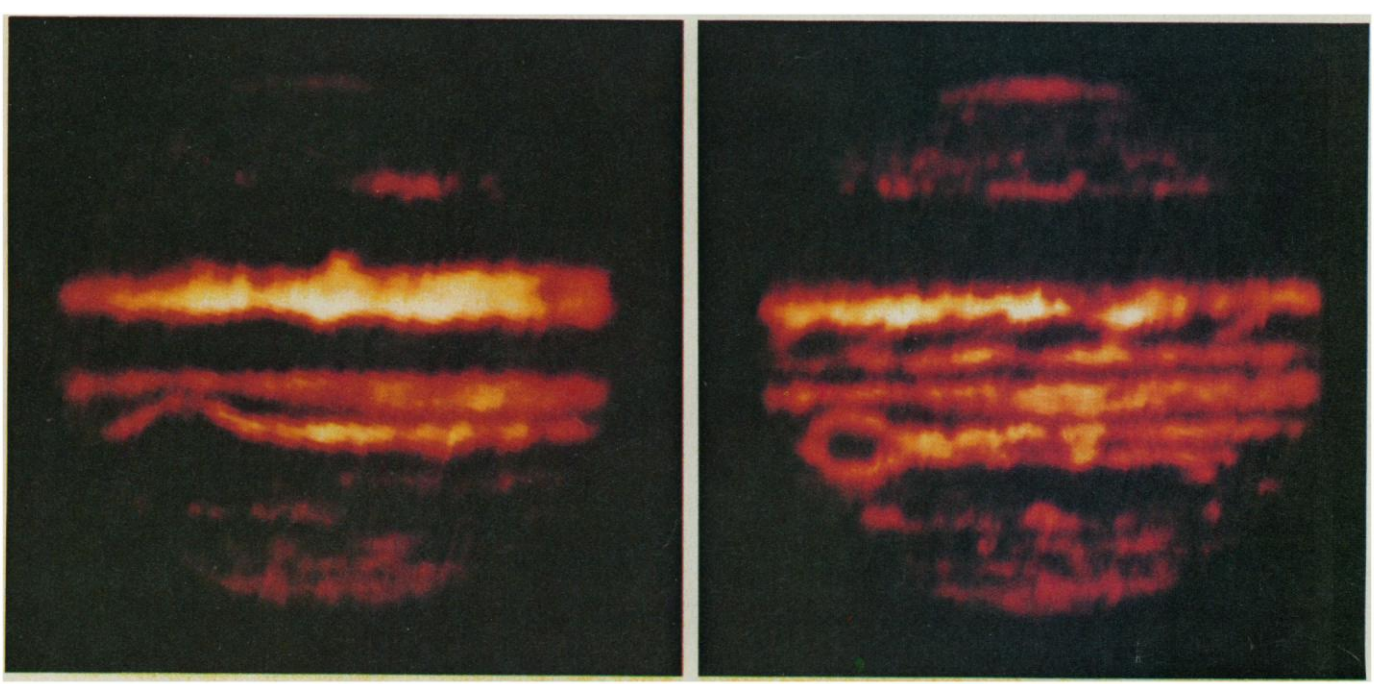

Fig. 1. Comparison of 5-μm images recorded at Palomar on 30 September 1978 (left) and 6 March 1979 (right). These images are shown in false color to bring out the large contrasts between the hottest areas (bright), warm areas (red), and the coldest regions (black). Hot 5-μm features indicate regions clear of overlying cold clouds. The Great Red Spot appears in the lower left of each image as a cold feature with warm regions defining its margin. Significant large-scale changes in warm belt regions can be seen between the two images.